ASTFE American Society of Thermal and Fluids Engineers

Proceedings of the 1st Thermal and Fluid Engineering Summer Conference, TFESC
August 9-12, 2015, Ne SAND2015-1360C

TFESC-12948

Contaminant Entrainment in a Liquid Fuel Fire

Alexander L. Brown and David L.Y. Louie

Sandia National Laboratories, PO Box 5800, Albuquerque, NM, 87185-1136, USA

ABSTRACT

Some fires may involve fuels that are contaminated with airborne particles such as hazardous chemicals or radioactive materials, and therefore pose a significant health risk by the potential inhalation of the contaminated material. In particular, consider a relatively inert solid material which is sub-micron in size that is suspended in a liquid solvent. Various mechanisms can lead to the solid becoming entrained in the air. First, as a liquid fuel is consumed it typically transitions through a boiling regime. As the vapor bubbles rupture at the liquid surface, the liquid response can result in the formation of film drops (collapsing bubble film) or jet drops (caused by liquid rapidly filling the vapor void). Surface wave action can also result in bubble formation and entrainment as the bubbles collapse. This mechanism is generally a function of wind speed and fluid properties. Also, mass may be entrained from a residual layer formed after consumption of the fuel. This paper reviews the existing literature on these entrainment mechanisms. Based on data from the review, the results from a Lagrangian/Eulerian coupled computational transport code are compared to some existing data on the entrainment of contaminants from liquid fuel fires. Since the multi-phase mechanistic prediction of the entrainment is not mature, the methods employ coupling of correlation data to the computational fluid dynamics (CFD) code.

KEY WORDS: Entrainment of Contaminated Liquids, Fire, Boiling liquids, Resuspension

1. INTRODUCTION

The evolution of airborne contaminants from a burning liquid is a well-established phenomenon, but mechanistic models are still being developed. While literature exists on the basic phenomenology, it has yet to be consolidated and verified in a way that provides confident predictions of fuel fire airborne release fraction (ARF) and respirable fraction (RF) for a variety of scenarios (see comparatively recent reviews by Kogan and Schumacher, 2008 and Bagul et al., 2013 [1,2]). The physical mechanism for entrainment is assumed to be drop formation from boiling bubbles that rupture at the surface of the liquid/gas interface. Two basic regimes exist for initial boiling. In the first regime, the drops are formed as the bubble dome collapses. This is commonly referred to as the film breakup regime. For fluids commonly studied such as water and salt water, this results in 1-100 μm diameter range drops. The second rupture entrainment mechanism is called the jet regime, and results from the rise and pinch-off of liquid tendrils as the liquid collapses around the bubble void after the film ruptures. This results in much larger drops, usually in the range of 100-300 μm diameter (Borkowski et al. 1986 [3]). According to the Department of Energy (DOE) handbook [4] for airborne release of particles in nuclear facilities, the film breakup regime is active for bubbles greater than 0.2 mm in diameter. The bubble mechanism is illustrated in Figure 1 on the left. On the right, the potential for wave action to create entrainment from stretching and collapsing waves is also illustrated. This alternate entrainment mechanism is understood to be highly dependent on the wind speed. Entrainment is also possible in the residual layer after the fuel has burned off, or from deposits on the surrounding surfaces.

*Corresponding Author: albrown@sandia.gov

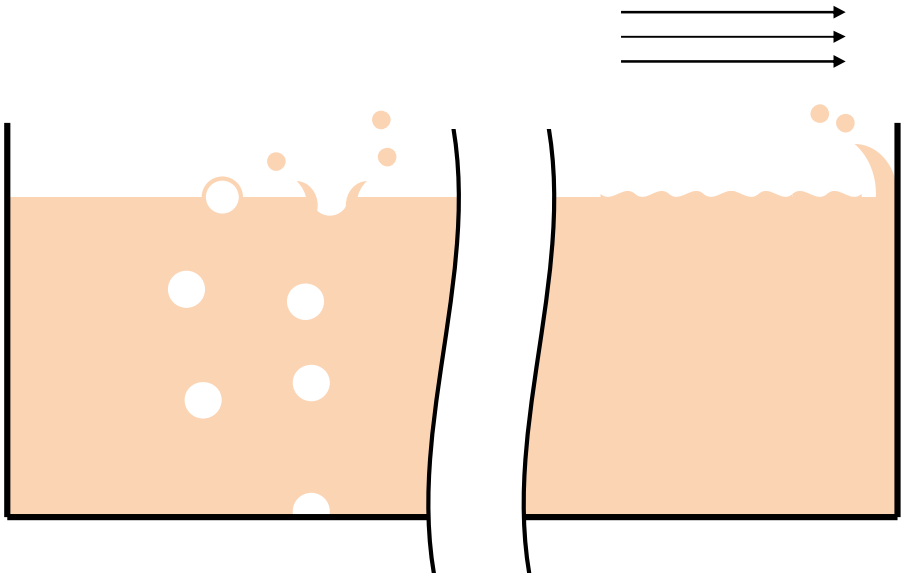

Fig. 1 An illustration of boiling entrainment (left) and surface wave entrainment (right) for liquid in air.

The DOE handbook [4] recommends the literature model from Kataoka and Ishii [5]. They reviewed an extensive quantity of literature and developed an analytical model for entrainment using an entrainment factor that is defined as the upward liquid mass flux divided by the upward gas mass flux. Kataoka and Ishii provide separate models for the entrainment in three distinct regions that are separated by a characteristic height. The near surface region entrains the most liquid mass, but the drops are mostly expected to fall back to the surface. For this regime, the entrainment factor is defined by the following:

$$E_{fg} = 4.84 \times 10^{-3} \left(\frac{\rho_g}{\Delta\rho}\right)^{-1.0} \tag{1}$$

This relation is described as valid in the range:

$$0 \le h^* \le 1.038 \times 10^3 j_g^* N_{\mu g}^{0.5} D_H^{*0.42} \left(\frac{\rho_g}{\Delta\rho}\right)^{0.23} \tag{2}$$

The entrainment factor is defined as the upward liquid mass flux divided by the upward gas mass flux:

$$E_{fg} = \frac{\rho_f j_{fe}}{\rho_g j_g} \tag{3}$$

Where ρ_f is the fluid density, ρ_g is the gas density, j_{fe} is the superficial liquid velocity (droplets), and j_g is the superficial gas velocity. Dimensionless parameters used in the formulation include:

$$j_g^* = \frac{j_g}{\left(\sigma g \Delta\rho / \rho_g^2\right)^{1/4}} \tag{4}$$

$$h^* = \frac{h}{(\sigma / g\Delta\rho)^{1/2}} \tag{5}$$

$$N_{\mu g} = \frac{\mu_g}{\left[\rho_g \sigma (\sigma / g\Delta\rho)^{1/2}\right]^{1/2}} \tag{6}$$

$$D_H^* = \frac{D_H}{(\sigma / g\Delta\rho)^{1/2}} \tag{7}$$

Here, σ is the surface tension, g is the acceleration of gravity, ρ is density, with the 'g' subscript implying gas. $\Delta\rho$ is the density difference between the gas and liquid, D_H is the vessel diameter, μ_g is the gas viscosity, and h is the height above the pool surface.

Equation 1 provides the correlation for boiling entrainment the first of three regions. The credibility of these relations is based on comparison to historical data, and self-similarity arguments, which are described in more detail in Kataoka and Ishii [5]. The other relations are for higher dimensionless heights, but the one presented here is the most generally applicable because it pertains to all pools in the near surface region. Curiously, the entrainment parameter does not involve any of the dimensionless parameters. It is only a function of the gas density and the difference in density between the gas and liquid. There are two fit parameters, the exponential factor and the pre-exponential factor. For most air and water systems, the exponential term will simplify to around 1000, which means that the mass of liquid entrained will be about five times the gas entrainment. This appears to be ridiculous because the gas is unlikely to drive more liquid than it weighs itself. The resolution to this issue is to note that the entrainment at the near surface level is superficial. In other words, the drops formed are simply formed, not necessarily ejected and entrained. In fact, much of the mass will fall back to the surface. Thus, it is tacitly understood that it is possible that the mass entrained through this mechanism will have undergone near-surface entrainment frequently before it actually entrains and departs. This means that the liquid on average becomes airborne several times before it is finally evaporated or entrained and transported away from the pool.

Since the DOE handbook [4] was published there has been a moderate amount of follow-on work for estimating entrainment phenomena. Cosandy et al. (2003, 2001) [6,7] measured entrainment of soluble and non-soluble contaminants in water. Spiel (1997, 1998) [8,9] measured saltwater entrainment from bubbles bursting at a surface. New analysis and simulation methods have also been reported. Duchemin et al (2002) [10] performed a numerical study of jet formed drops. Koch et al. (2000) [11] use a surface marker particle method for predicting the dynamics of a multiphase solution to the Navier Stokes equations. Zhang et al. (2012) [12] present a new formula for predicting the number of jet drops emerging from a drop based on dimensionless analysis. A modified formula for determining the critical drop diameter for jet formation is also proposed. Zhang et al. include data from water as well as molten metal bubbles in the formulation, and provide a correlation for highly varying conditions. Correlations for the height of the rising jet and the height of drop ejection can be found in Bagul et al. [2]. While models exist for some phenomena, none of the separate capabilities have been consolidated in a generalized model as was done in Kataoka and Ishii [5]. Accurately modeling the entrainment of drops from a boiling surface remains a difficult problem.

After a liquid fire is extinguished, there may be a residual layer. A non-volatile contaminant may be found in high concentration in the residual layer. Deposition may also occur on surrounding surfaces resulting in subsequent entrainment. These phenomena have been reviewed recently by Henry and Minier [13]. These phenomena are complex, and further complicated for conditions that do not involve idealized single-component round particles. Atomic forces become relevant to the behavior, and wind, surface thermal stress, and morphology may also be complicating factors. A residual layer may entrain mass well after fuel has been consumed in the case of a contaminated liquid fuel fire. Resuspension is an important phenomenon relating to contaminant air entrainment, but this study will focus on physics that occur earlier in the problem of interest.

The work reported herein describes an effort to model the entrainment of contaminated liquid fuel using a computational fluid dynamics (CFD) reacting flow code. The long-term goal is to demonstrate and build confidence in predictive tools to aid in the assessment of risks and hazards associated with the entrainment of contaminated liquids. In this paper, experiments of Mishima and Schwendiman (1973) [14] are simulated to assess the ability of modern simulation tools to make quantitative predictions of reported experiments. For convenience, Mishima and Schwendiman may be abbreviated MS later on in this report. The MS work

constitutes some of the primary data that are relied upon for facility safety in the DOE handbook. The effort highlights some important physical phenomena that need to be simulated to have confidence in model predictions. The increased fidelity of information from the model underscores a need to better understand the phenomenological nature of these events.

2. METHODS

As described above, there are models and correlations for predicting mass flux from a boiling surface. We are motivated to use the methods of Kataoka and Ishii [5] primarily because the relations are suggested in the DOE handbook. Another component of this same problem is the particle size distribution. This is a complex problem, and models for this are not as prominent or well characterized. The flow dynamics near the boiling surface are complex due to the jetting of gases following the rupture of the bubbles. The problem of drop evolution from a boiling surface is not well resolved. There are numerous studies on the size of drops formed from boiling systems. No study has been found that brings together all the components needed to apply the models at the boundary of a CFD code.

With a relationship for the entrainment mass defined in Equation 1, injection velocity spatial location, and size distribution are the remaining factors needed to fully describe the system input. Boiling data from Borkowski et al., (1986) comprise a component of the drop size data presented and recommended by the DOE handbook. Different size data exist for different bubble sizes. Size distribution plots in terms of drop number frequency are presented, and the distribution is bi-modal. The smallest drops form in the film region, and result from the rupture of the surface bubble. The largest drops come from the jet region, and result from the collapse of the bubble and the rebound of the cavity mass. Figure 2 shows a plot of the size distribution for a 1.4 mm bubble of a 0.1% NaCl-Water solution. The plot is an extraction from the presented distribution, and reflects the model that is to be used subsequently. The extraction points are treated as interpolation points, and the model for the distribution is generated by sampling drop sizes probabilistically, generating drops that reflect the mean mass and diameter with respectable accuracy. A computational script was written to sample the data from this report and generate a tabulated list of input particles that would be distributed in space and time such that the mass and number mean from the Borkowski et al. data are well represented. The mass mean particle diameter was approximately 130 μm, and the number mean was around 3-4 μm.

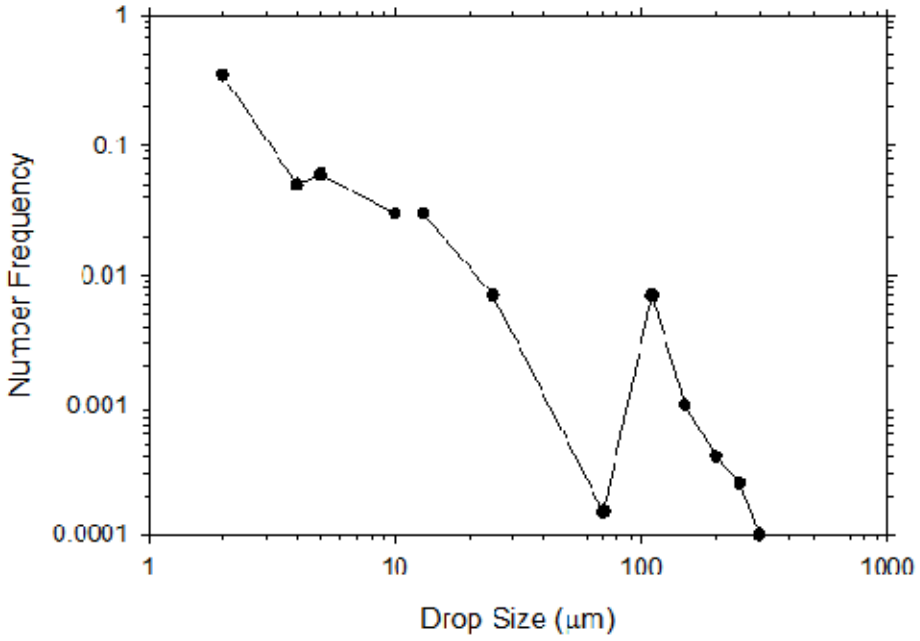

Fig. 2 An extraction of the number frequency data from Borkowski et al. (1986)

The experiments of Mishima and Schwendiman (1973) [14] involve the burning of a beaker filled with kerosene and 30% tributyl phosphate (TBP) contaminated with various materials. Iodine was one of the contaminants, and was found to volatilize and was therefore more prone to become airborne. The other contaminants (including the TBP) were not volatile, and yielded similar results to each other, suggesting that the primary method of evolution was by drop transport. They pre-heated the liquid to the boiling point, and then ignited the fuel in a 50 mL beaker. We assume a standard dimension from current commercial product data of 56 mm height and 42 mm outer diameter for the beaker.

Additional assumptions are required to perform the simulation. Boiling was assumed uniform over the surface of the liquid, resulting in a uniform spatial release of particles. The tests typically lasted 50 minutes, over which time the liquid level receded from about 20 mm above the bottom of the beaker to near the bottom (4-9 mL of residue remained according to the test report). Since receding liquid (i.e. modeling with a moving computational mesh) is not a current capability of the simulation tools, simulations were performed for a short time with the liquid layer near maximum and minimum points to assess the trends. The behavior of the system between the two steady-state conditions can be estimated by interpolation between the two modeled conditions. Because the evaporation model did not allow for differing evaporation potential for multiple constituencies, the particles were assumed to be non-evaporating drops. The baseline turbulence parameters at the inlet are presumed to be negligibly low (described in more detail later in Table 1), and the inlet velocity of the drops is assumed to be random between 0-1 m/s. Simulations are initialized with the beaker initially full of air at ambient condition. The fuel evaporation is modeled as a constant flow rate of fuel from the liquid surface (7×10^6 kg/sec).

SIERRA/Fluid Mechanics is a suite of predictive tools that have been developed by the Advanced Simulation and Computing (ASC) program. The SIERRA architecture enables calculations that take advantage of the massively parallel architecture computers at Sandia National Laboratories. The Fuego sub-module is designed to predict low-Mach number ($M<0.3$) reacting flows, and has a capability to model particle and drop transport using a dilute spray approximation Lagrangian/Eulerian coupling. The liquid phase can be modeled as individual Lagrangian drops that interact through momentum source terms with the Eulerian gas phase.

Particles are modeled with a parcel concept. Instead of modeling the transport of every unique drop, the model assumes that the general behavior can be appropriately modeled by statistically grouping like-sized particles and transporting the mass together. The parcels greatly facilitate modeling the system as many of the fine drops have little individual effect on the flow, and can be transported in bulk. Thus, the particles are transported in a more efficient way that statistically represents the bulk behavior. Particles that impact a surface are assumed to stick. No collisional effects are presently modeled. A drop vaporization model exists, but is not used in this case under the assumption that the burn rate is completely described by the gas evolution at the surface of the fuel. This facilitates quantitative comparison. Mass entrained and exiting the system is assumed to have a proportional amount of contaminant to the initial mixture. The liquid evolution from the surface is assumed to contain a proportional amount of contaminant to the initial mixture. Reactions are modeled with the eddy dissipation concept (EDC) model of Magnussen [15].

The above presented models for drop size and mass are used to generate drops that emerge at the surface of the burning fuel. The last factor necessary to model the behavior of these drops is the turbulence source terms at the inlet boundary. Turbulence is treated as a free parameter, and is described more in detail below in the context of the results.

3. RESULTS AND DISCUSSION

Figure 3 shows predicted flame temperatures and particles (exaggerated for visibility) based on modeling performed with the SIERRA/Fluid Mechanics code. Significant deposition is predicted on the sides of the beaker, as speculated in the data report. The initiation of the fire results in significant entrainment. Entrainment decreases as the fire matures. Smaller particles are more likely to be entrained, while the larger particles are

more likely to fall back to the surface of origin. The larger particles tend not to rise as high because gravity is a more significant force relative to the other forces on the particle with increasing size.

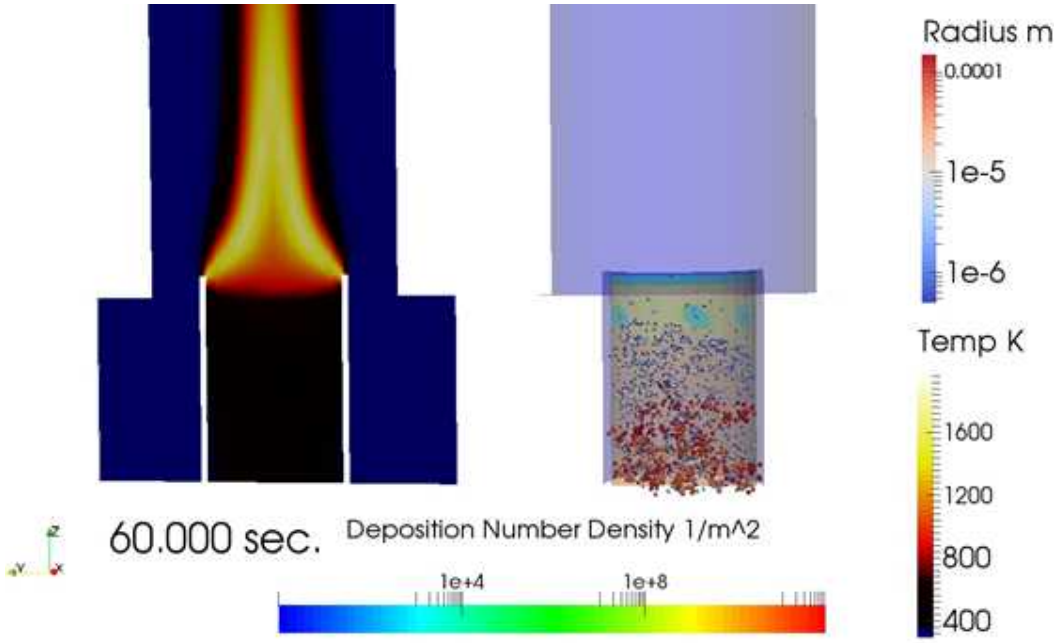

Fig. 3 An illustration of the predicted liquid entrainment from the MS [14] tests with particle parcel sizes exaggerated for visibility. Temperatures are plotted on the left, and particle parcels are exaggerated in size and colored according to their size with the hemispheric-cut semi-transparent surface sides of the beaker colored by number deposition density.

The first set of simulated results helped define subsequent analyses. The ultimate destination for the particle mass is initially calculated for two ten minute intervals for a baseline scenario. The first interval is the starting 10 minutes. This interval predicts the behavior of the system during start-up conditions. After about a minute, a steady-state fire condition is attained where the fire is burning regularly, and the deposition of drops becomes steady. The mass of drops from the boiling fuel surface to deposit on three key surfaces is shown in Figure 4 for the early time interval. The significant part of this plot relative to the MS [14] data is the "escaped" mass, which is essentially all released in the first few seconds after ignition. This is due to the transient nature of the start-up, allowing more particles to escape as the flame dynamics occur nearer the fuel surface. The mass deposition for the last ten minutes simulated with the pool depth near the bottom of the beaker is shown in Figure 5. In this simulation, the end time was simulated by tracking the constant particle rate as it interacts with a constant fire at increased depth. The simulation was intended to explore the steady-state deposition towards burn-out to provide a basis for estimating the long-term trend (by interpolation). It was thought that the initial transient information from this simulation would not be used. It was observed that the magnitude of the initial pulse was approximately the same as for the scenario at the first 10 minutes. Because of this and the fact that the initial pulse involved most of the entrained mass was surprising, further evaluation of this finding was warranted. Visualization (like Fig. 3, but not herein reproduced) of the results suggests that the very small particles continue to escape after the initial transient.

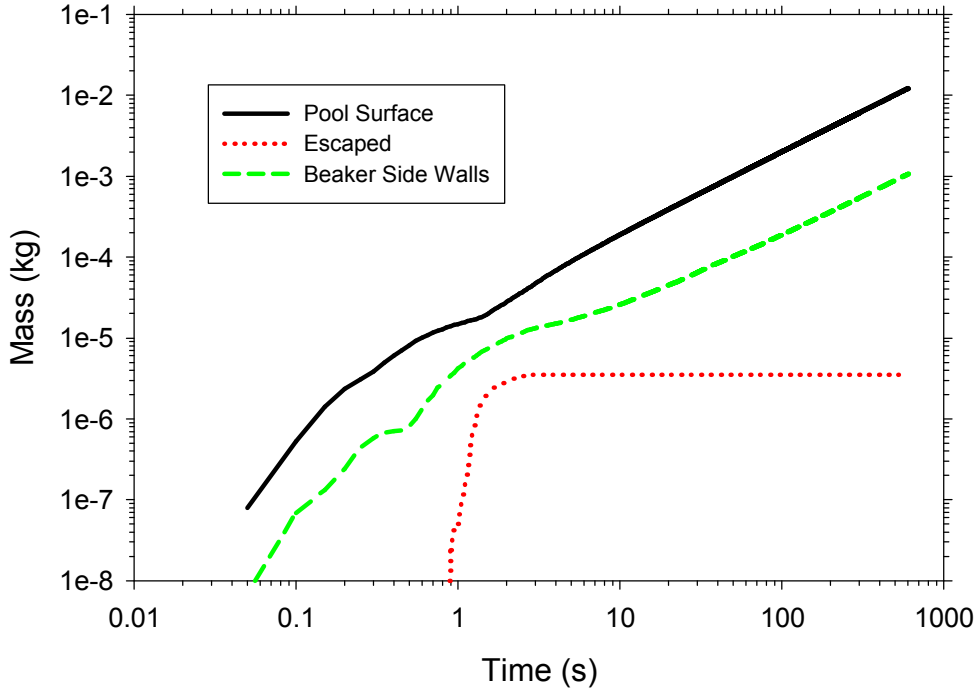

Fig. 4 Predicted mass deposited for the first 600 seconds (20 mm height pool).

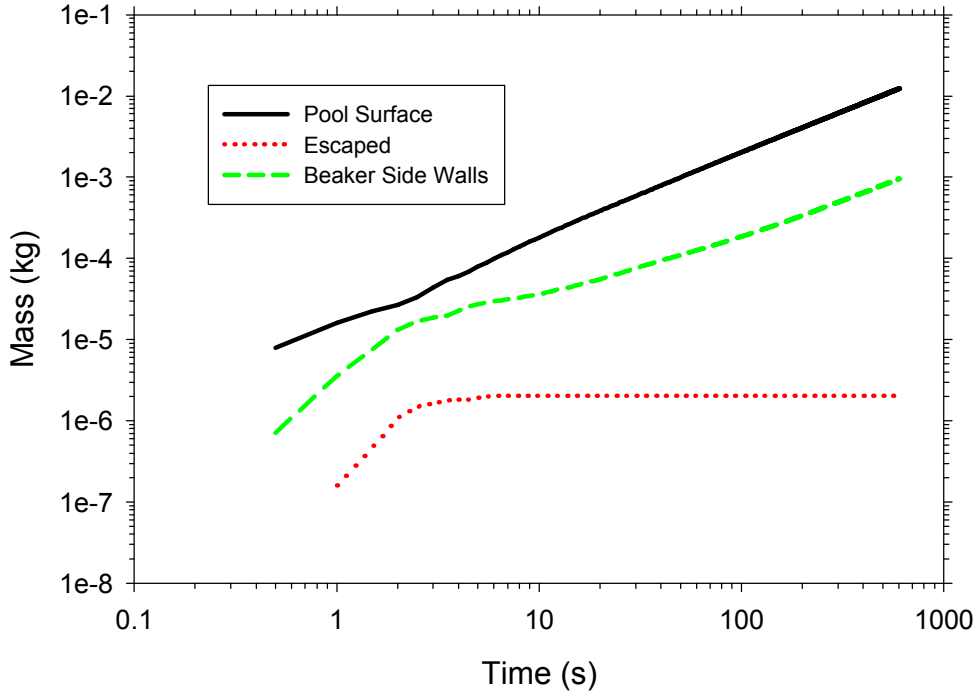

Fig. 5 Predicted mass deposited for the final 600 seconds (0 mm height pool).

Figures 6 and 7 show the deposition based on number of particles. Unlike the mass deposition in Figures 4 and 5, the particle count suggests that there is still escape of some particles following the initial transient. The escaping particles are quite small, and are not significant enough in mass to contribute to the mass deposition. These plots also suggest that the deposition rate of particles becomes relatively steady after the initial transient.

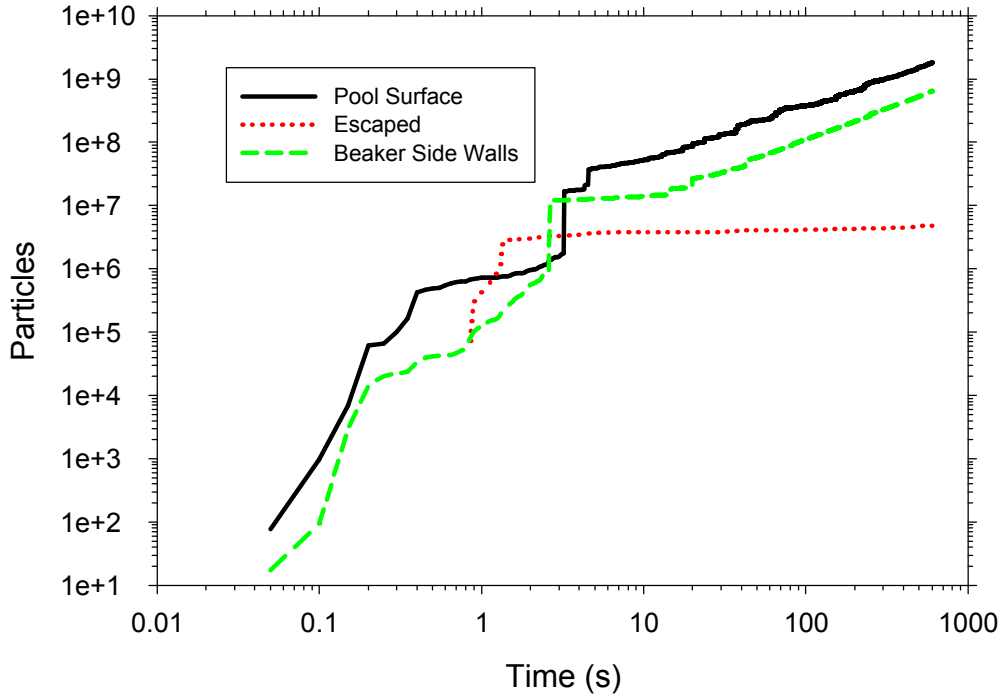

Fig. 6 Predicted particle number deposited for the first 600 seconds (20 mm height pool).

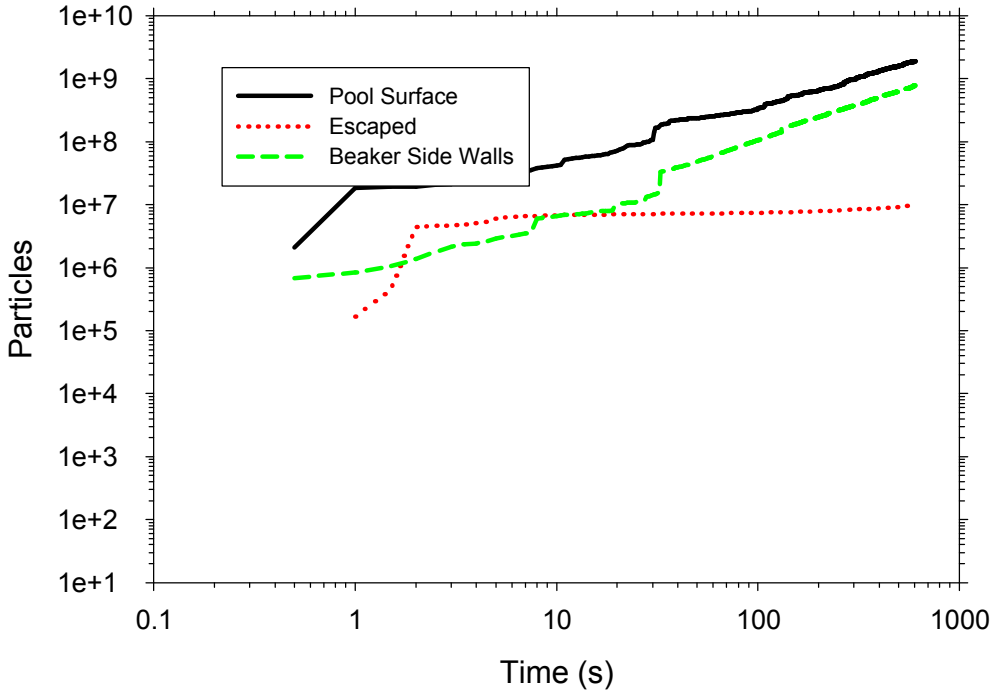

Fig. 7 Predicted particle number deposited for the final 600 seconds (0 mm height pool).

A large amount of the particle mass is found deposited on the beaker side walls. This occurs as the drops formed from the boiling liquid impact the side walls. The deposited mass in the actual tests might subsequently react to evaporate off the walls, but might also through gravitational forces descend back to the pool surface. Entrainment from deposition on the beaker walls was postulated by the authors of the

experimental test report as being a potentially significant source of entrainment of contaminant particles. This computational work in the magnitude of the predicted deposition indicates agreement that this mechanism for entrainment is potentially significant.

This first round of simulations helped determine the subsequent models that were run. It was noticed that the first 6 seconds was when almost all of the particle mass exited the beaker to the collection point. Almost no mass was subsequently collected. This suggests that the initial transient was the driving factor in the total release. This finding was not anticipated, as the experimental report did not suggest this to be the case. It was thought that the longer transient would result in a more significant emission. The main purpose for initially running the two liquid heights was to extract the effect of the liquid height on the steady emission of particles over the duration of the flaming. Comparing Figure 4 and 5 it is also apparent that the simulation for the final 10 minutes (which has a lower liquid layer in the beaker) resulted in a comparable initial emission of particle mass. This is thought to be due to the buoyant effect of flames initiated deeper in the container. The increased motion of the flames is better able to lift particles, even though the particles have farther to go to exit the beaker. This raises the question of whether the experiment was a conservative test because there was no effort to vary the initial liquid height. A couple of different particle input files were employed, and we also noticed that the magnitude of the initial 6 second mass escaping the beaker depended on the particulars of the input file. This likely has to do with the precise spatial distribution of particles relative to the flame during the initial flame ignition. The main difference in the particle input files was in the location of individual particles as a function of time, and could be viewed as a good model for the actual physical uncertainty in this regard. There was negligible difference in the particle size distribution. The sensitivity to different particle input files and to the initial liquid height were therefore selected as parameters of variation for further investigation.

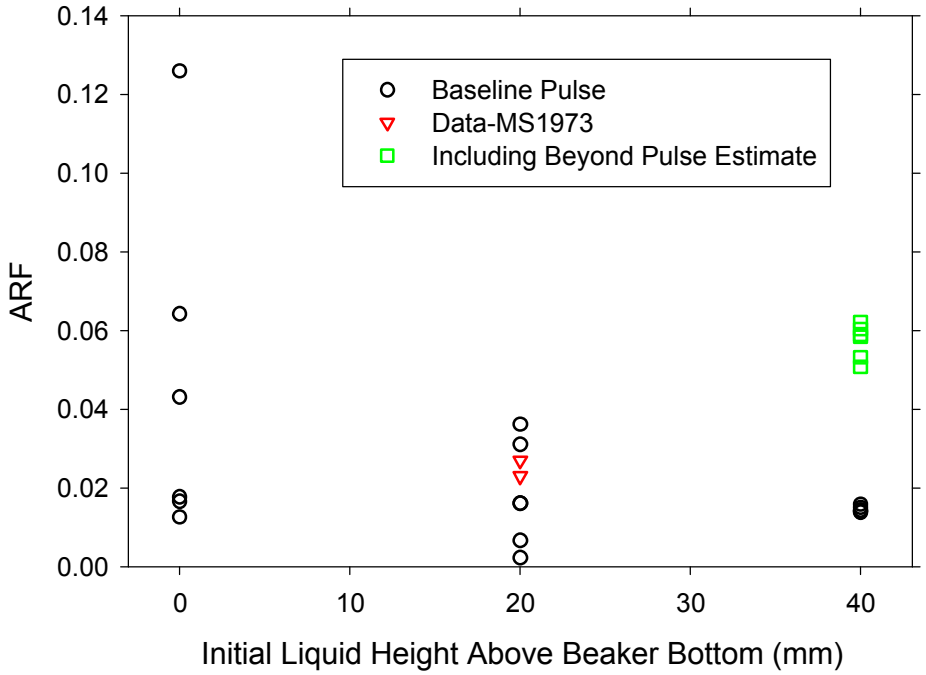

Fig. 8 Summary ARF plot for the baseline turbulence assumption for various particle input files and initial liquid heights.

For the baseline turbulence scenario, the initial liquid height above the bottom of the beaker and the particle input file were varied. The results are plotted in Figure 8 in terms of airborne release fraction (ARF) for consistency with the data. The data were for a single initial liquid height. There is a general increase in ARF with a decrease in the liquid height for baseline pulse simulations. The simulations with 40 mm initial height had the lowest ARF from the pulse, but particles were increasingly able to entrain in the plume at that

height. Simulations were run to 160 seconds, and the trend for 60 seconds from 80-140 seconds was projected out to the full 50 minute duration by linearly interpolating the entrainment trend from the 40 mm height value during the first minute out to the zero value obtained for the steady-state emission case where ignition occurred with the liquid height 20 mm above the bottom of the beaker. The green squares indicate the ARF that is projected using this method, and represent the sum of the baseline pulse data and an estimate of the ARF due to the steady entrainment over the course of the burn. The baseline pulse data for the 20 mm initial height case exhibits a greater spread than the data, but generally agrees with the mean.

The particle transport model uses a stochastic function that is scaled by local turbulence parameters to model the effect of sub-grid turbulence on the transport of the particles. Turbulence was modeled in these cases with the temporally filtering of the Navier Stokes (TFNS) model [16] that is in the class of turbulence models that are a hybridization of large-eddy simulation (LES) and Reynolds averaging of the Navier Stokes equations (RANS) methods. Sub-grid turbulence that is postulated to be present due to the agitation of the boiling liquid/gas interface is believed to contribute to particle motion. Characteristic length-scales of turbulence might vary from the smallest postulated boiling drop size (around 0.5 mm) up to the internal diameter of the beaker (40 mm). Turbulence intensity (fluctuating velocity over the mean) is difficult to assess, but may be significantly higher than unity because it is augmented by the rupture of bubbles at the surface of the liquid and the motion in the cylinder. The local contributing velocities may be much higher than the bulk mean flow of fuel vapor. The initial tests used the low baseline values in Table 1 as boundary conditions at the fuel surface. Subsequent analysis included four variations labeled from A to D as indicated in Table 1. This was to ascertain whether the finding that the main particle emissions were due to the initial transient held over a range of possible turbulence conditions.

Table 1 Turbulence parameters for the sensitivity study

Runs	**k** $[m^2/s^2]$	**epsilon** $[m^2/s^3]$	**Corresponding length scale** [m]	**Corresponding turbulence intensity** [%]
Baseline	5.95e-7	4.56e-7	1.6×10^{-4}	100
A variation	5.95e-5	1.53e-4	5×10^{-4}	1000
B variation	5.95e-5	1.92e-6	5×10^{-4}	1000
C variation	5.95e-3	1.53e-1	4×10^{-2}	10000
D variation	5.95e-3	1.92e-3	4×10^{-2}	10000

The six scenarios with baseline turbulence are plotted again with the data in Figure 9 (20 mm height). This plot also includes eight scenarios where the turbulence parameters were varied according to values in Table 1. Of particular interest was whether changing the turbulence parameters had an effect on the longer-term entrainment. In Figure 9, the long-term entrainment is plotted with the initial pulse ARF. The contribution of the long-term entrainment is expressed in red with a stacked bar. There were only two cases where this long-term entrainment was found to be significant (above 1% baseline ARF). These were both related to turbulence case D. The different numbers denote different particle input files. Particle input file 7 uniformly resulted in higher predicted ARF than particle input file 8 for all turbulence assumptions.

These simulations suggests that the turbulence parameters can result in a higher release. The combination of parameters used where the release was significant involved high turbulence intensity as well as a large characteristic length-scale. Other more moderate conditions did not exhibit significant entrainment.

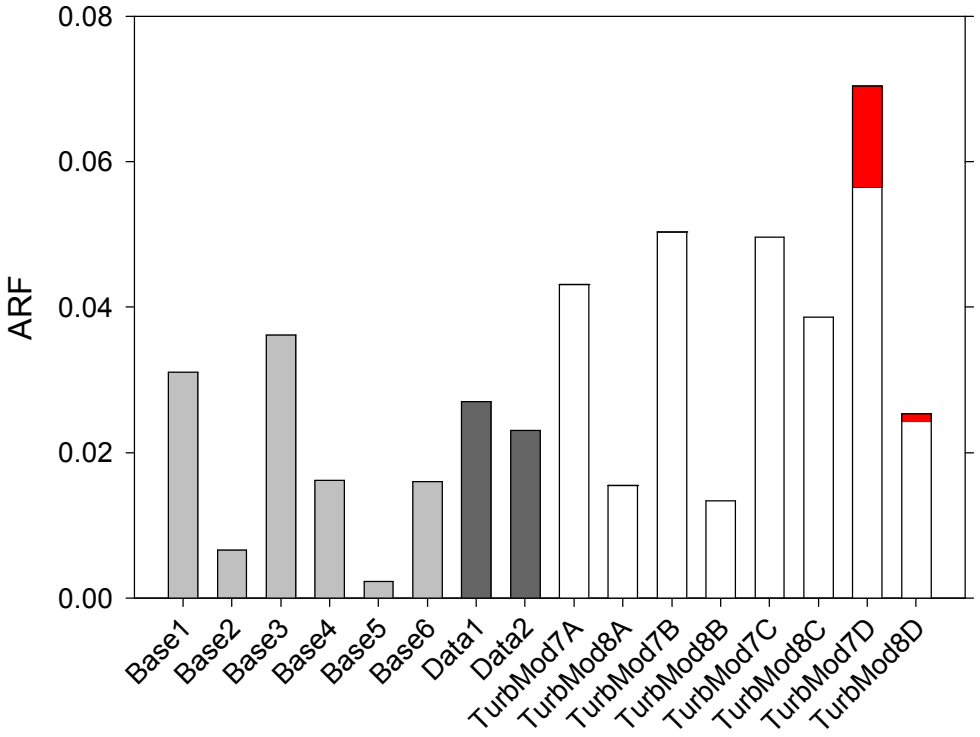

Fig. 9 ARF for a 20 mm initial height for a variety of particle input files (the simulation number) and turbulence assumptions (the simulation letter) compared to the data. Red bars correspond to the long-term entrainment due to turbulent transport.

4. GENERAL DISCUSSION

The models employed in this exercise gave predicted ARF values that were on average reasonably close to those measured experimentally. This could be viewed as a validation of the predictive codes. This interpretation of the results is not how the authors believe that the results are best interpreted. There were several assumptions made that are believed to have a significant effect on the quantitative results of these simulations. First, the quantitative predicted ARF comes primarily from the initial burst in the first few seconds of simulation for most of the cases. Ascribing accuracy to this part of the simulation is not warranted. The method of ignition was not stated in the experiments, and is therefore believed to be most probably based on a match or lighter manually inserted at ignition time. Furthermore, since the liquid was heated to the boiling point prior to ignition, the beaker in the experiments was probably not filled with air down to the liquid level as it was our simulation. The simulation initial conditions used in the model were convenient and reflected the uncertainties to within those reported experimentally. In follow-on work it might make sense to try different computational initial conditions to see how sensitive the predicted ARF is to the initial gas phase fuel in the beaker. It might also be warranted to perform new experiments that resolve the temporal contribution to the ARF. The experimental results were integrated over the duration of the test.

Another point of concern is that the liquid drops in the model were not allowed to evaporate. The reason for this assumption is that some minor code modifications are necessary for this capability to exist in the current code. Such modifications are being considered for subsequent development. A viable entrainment mechanism may involve evaporation of the fuel from around the contaminant. The initial formation of a drop may occur followed by the evaporation of the volatile component, and then the transport and escape of the residual (much smaller and more prone to escape) material. It is possible that this mechanism is a dominant mechanism, in which case the negligible mass entrainment after the initial pulse might become more significant as the particle size distribution shifts downward and the density of the contaminant in the

particle increases. It would be helpful to re-visit these simulations with the model improvements to better reflect the potential for a downward shift in the particle size due to evaporation. A method would need to exist to capture the varying mass of the different particle constituencies at the outflow boundary in this case.

The authors of the experimental report (MS; [14]) postulate that the deposition on the beaker side-walls and subsequent drying and entrainment might be an active mechanism for contaminant release. These prediction results show that the beaker side walls do indeed experience significant deposition of drops. The subsequent mechanistic behavior was not modeled, but remains a viable consideration.

A third point of concern is the fact that these data are being used in regulatory space to define a conservative ARF. The DOE handbook uses bounding values including data from this test as a guideline for designing safety systems and risk assessment. The simulations in this exercise suggested a significant relationship between ARF and the initial height of the liquid layer. The best predictions at this point suggest that the initial liquid height was not a particularly conservative selection, as both higher and lower initial levels resulted in increased mean ARF values both compared to the predicted and experimental ARF mean at the conditions of the experiment. Performing a revised set of experiments with this in mind at a greater variety of representative conditions would greatly increase the confidence level in the recommended regulatory and design limits. If the model reaches a point at which quantitative confidence can be ascribed to the results, it may obviate the need for further testing.

Even though the modeling methods employed in this effort are lacking for a complete description of the behavior of this complex system, the exercise has uncovered important considerations that should be noted in future studies of these phenomena. Surface boiling and entrainment models are not particularly mature. Although there is not a generalized model for phenomena of this nature, there are models and data that can be combined to provide reasonable assumptions for simulating the transport of the drops. Simulations suggest particle size filtering occurs below the flames that preferentially entrains the smallest particles into the flames and into the plume. This suggests that the film rupture mechanism for particle formation is important, as it produces the smaller drops that are more likely to be entrained. Jet-formed drops may also be important during initial or transient events, and if they can evaporate to the point that they become small. This behavior can be explored in future work after implementing a multi-component evaporation model.

6. CONCLUSIONS

These simulation results suggest that the airborne release of contaminants from a contaminated burning fuel in the case of these experiments was primarily due to the initial flame dynamics during the start of the fuel burn. Subsequent entrainment was subtle by comparison. No data exist to substantiate this finding, but the range of potential turbulent transport under steady conditions is thought to be adequately evaluated. The steady-state entrainment was negligible except in a few cases where the intensity of the turbulence was augmented. New data in this regard would be helpful.

Varying the initial pool height resulted in scenarios with increased airborne release of contaminant in the models. This was not varied in the experiments, and the data from the experiments are being used as a conservative regulatory guideline. It is advisable to conduct additional tests informed by simulations that better capture the conservative conditions for this type of scenario by varying the initial height of the pool. These experiments, while helpful, might not be bounding experiments for cases where the fuel height varies.

This comparison effort suggests the need for higher temporal fidelity datasets to better substantiate the mechanistic predictions of contaminant release for boiling pool fires. Data on the turbulence above the boiling pool surface might also be helpful, although results were not particularly sensitive to this parameter.

Some minor model improvements would greatly enhance the ability to model the physics of this scenario, as well as the confidence in the predicted results. Accurate multi-component particle capabilities might be expected to yield results that show the long-term entrainment to be more significant than it was in these simulations. Resuspension from surface deposits might also be important to the quantitative risk.

ACKNOWLEDGMENT

Sandia is a multiprogram laboratory operated by Sandia Corporation, a Lockheed Martin Company, for the United States Department of Energy under Contract No. DE-AC04-94AL85000. Document reviews by Fred Gelbard and Flint Pierce are appreciated. This work was funded by the DOE NSRD program under WAS Project No. 2014-AU-2014033.

REFERENCES

[1] Kogan, V., Schumacher, P.M., "Plutonium release fractions from accidental fires," *Nuclear Technology*, 61, pp. 190-202, (2008).
[2] Bagul, R.K., D. S. Pilkhwal, P.K. Vijayan, and J.B. Joshi, "Entrainment phenomenon in gas-liquid two-phase flow: A review," *Sadhana*, 38(6), pp. 1173-1217, (2013).
[3] Borkowski, R., Bunz, H., and Schoeck, W., "Resuspension of Fission Products during Severe Accidents in Light-Water Reactors, KfK3987, EUR 10391, May (1986).
[4] Department of Energy, DOE HANDBOOK: Airborne Release Fractions/Rates and Respirable Fractions for Nonreactor Nuclear Facilities, Volume 1 and 2, U.S. Department of Energy, DOE-HDBK-3010-94, Reaffirmed 2013 (2013).
[5] Kataoka, I., and Ishii, M., "Mechanistic Modeling and Correlations for Pool-Entrainment Phenomenon," NUREG/CR-3304, ANL-83-37, April (1983).
[6] Cosandey, J.O., von Rohr, P.R., "Entrainment of soluble and non soluble tracers from a boiling water surface," *Nuclear Engineering and Design*, 208, pp. 87-97, (2001).
[7] Cosandey, J.O., Günther, A., von Rohr, P.R., "Transport of salts and micron-sized particles entrained from a boiling water pool," *Experimental Thermal and Fluid Science*, 27, pp. 877-889, (2003).
[8] Spiel, D.E., "More on the births of jet drops from bubbles bursting on seawater surfaces," *Journal of Geophysical Research*, 102(C3), pp. 5815-1521, (1997).
[9] Spiel, D.E., "On the births of film drops from bubbles bursting on seawater surfaces," *Journal of Geophysical Research*, 103(C11), pp. 24907-24918, (1997).
[10] Duchemin, L., Popinet, S., Josserand, C., Zaleski, S., "Jet formation in bubbles bursting at a free surface," *Physics of Fluids*, 14(9), pp. 3000-3008, (2002).
[11] Koch, M.K., Voßnacke, A., Starflinger, J., Schütz, W., Unger, H., "Radionuclide re-entrainment at bubbling water pool surfaces," *J. Aerosol Sci.*, 31(9), pp. 1015-1028, (2000).
[12] Zhang, J., Chen, J.J.J., Zhou, N., "Characteristics of jet droplet produced by bubble bursting on the free liquid surface," *Chemical Engineering Science*, 68, pp. 151-156, (2012).
[13] Henry, C., Minier, J.-P., "Progress in particle resuspension from rough surfaces by turbulent flows," *Progress in Energy and Combustion Science*, 45, pp. 1-53, (2014).
[14] Mishima, J., and Schwendiman, L.C., "The Fractional Airborne Release of Dissolved Radioactive Materials During the Combustion of 30 Percent Normal Tributyl Phosphate in a Kerosine-Type Diluent,"BNWL-B274, June 1973.
[15] Magnussen, B.F., "On the Structure of Turbulence and a Generalized Eddy Dissipation Concept for Chemical Reactions in Turbulent Flow," 9th AIAA Sc. Meeting, St. Louis, (1981).
[16] Tieszen, S.R., Domino, S.P., and Black, A.R., "Validation of a simple turbulence model suitable for closure of temporally-filtered Navier-Stokes equations using a helium plume," SAND2005-3210, June 2005, Sandia National Laboratories.